TUNING PROCEDURE OF THE 6-METER IPHI RFQ

Olivier Piquet, Michel Desmons Alain France (CEA Saclay, F91191 Gif-sur-Yvette, France)

Abstract

In the framework of the IPHI project (High Intensity Proton Injector), the RFQ cavity is divided into 6 sections of 1 meter each, which are assembled in 3 coupled segments. We present the tuning procedure of the IPHI aluminium cold model, that is (i) adjusting coupling capacitances and dipole rods for optimum stability and (ii) tuning the 96 slugs to achieve constant inter-vane voltage. Fields inside RFQ quadrants are measured by a fully automated bead-pull system. Tuning this 6-meter long cold model is a comprehensive training in view of the future tuning of the copper RFQ with the variable voltage profile.

THE IPHI COLD MODEL

A 6-meter aluminum cold model has been built to validate the tuning procedure of the IPHI RFQ. To tune it, several devices have to be adjusted at different steps of machining and assembling.

The cold model can be divided in 2-meter long segments with capacitive coupling in-between which can be set by additional shims (Figure 1). The tuning of the segment end regions is made by machining the thickness of the end and coupling plates, and by dipole rods length adjustments. Finally, irregular tuners distribution and RF inputs will be used to achieve the setting of the inter-vane voltage. Here, we will work with 24 slug tuners and 2 RF ports (used as slugs) per quadrant for the tuning procedure of the model (Figure 2).

Moreover a fully automated test bench has been developed to measure the field distribution [1]. Based on the perturbation method, a bead is guided successively through 4 quadrants and field distribution of excited mode is obtained. This test bench will be used to identify modes for the stability analysis and then for the tuning process of a constant voltage profile.

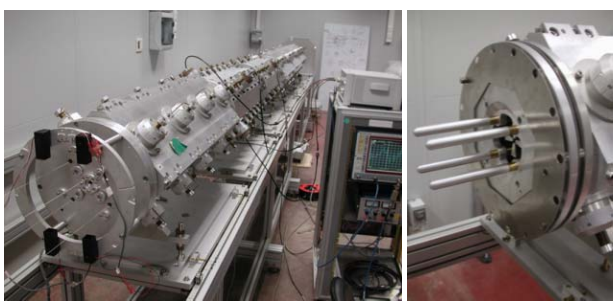

Figure 1 left: cold model with test bench Right: coupling cell with dipolar rods and 0.8mm shims on either side

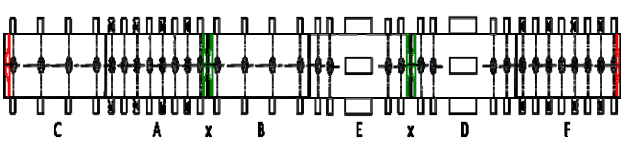

Figure 2: 6-meter cold model. C,A,B,E,D and F: 1-meter sections names; X: coupling cell.

4-WIRE LINE MODEL

Eigen-Value-Dependent Boundary Conditions.

A loaded, lossless 4-wire transmission line model [2] is used to relate differences between measured and desired inter-vane voltages, to tuning devices dimensions (dipole rods, end plates, coupling plates, and slugs). Voltages between adjacent vanes $u = |u_1,u_2,u_3,u_4|$, expressed in $U = |U_Q,U_S,U_T|$ basis

$u_1:=+U_Q+U_S$, $u_2:=-U_Q+U_T$, $u_3:=+U_Q-U_S$, $u_4:=-U_Q-U_T$,

are solution of $-\partial^2U/\partial z^2 + AU = \lambda U$, where the A matrix contains line inductance and capacitance (derived from 2D simulations) vs. abscissa z, and $\lambda = (\omega/c)^2$. Boundary conditions (BC) are $\partial U_a/\partial z = -s_aU_a$, $\partial U_b/\partial z = +s_bU_b$, at RFQ ends $z = a$, $z = b$, and $\left|\partial U_{ci}^-/\partial z\right| = s_{ci}\left|U_{ci}^-\right|$ $\left|\partial U_{ci}^+/\partial z\right| \quad\quad \left|U_{ci}^+\right|$ at any coupling cell $z = c_i$. The operator thus defined has a pure point spectrum with real eigen-values [2]. Eigen-space is the direct sum of one quadrupole subspace with eigen-pairs $\{\lambda_{Qi},|V_{Qi}(z),0,0|\}$, and two dipole subspaces $\{\lambda_{Sj},|0,V_{Sj}(z),0|\}$ and $\{\lambda_{Tk},|0,0,V_{Tk}(z)|\}$. BC matrixes s_a, s_b and s_{ci} are directly proportional to equivalent circuit admittances. Quadrupole eigen-frequencies can be safely predicted with constant s values, because load terms are resonant ($s \neq 0$); then the differential problem is Sturm-Liouville (SL), and is straightforwardly solved by linear algebra techniques. The case of dipole modes is quite different, because rods make load either resonant (when rod length is an even number of quarter wavelengths–including 0), either anti-resonant (rod length being an odd number of quarter wavelengths). The field of solving SL problems with eigen-value-dependent BC is still open [3] [4]; however we may take advantage of the underlying microwave circuit: (i) Foster's reactance theorem [5] states that any realizable admittance y verifies $\partial\,\mathrm{Im}(y)/\partial\omega > 0$; (ii) Richard's theorem [6] states that the admittance of a microwave circuit is a rationale function of $\exp(2j\omega q/\nu)$, where q is the shortest commensurate-length line in the circuit, (ν = wave celerity). With (i), (ii), and the model of monopole antennas in mind, load BC can be expressed as $s(\omega) = \tan\sigma(\omega)$, where σ is a polynomial strictly increasing with ω. The SL problem may be solved continuously vs. ω, and its eigen-values $\lambda_{Qi}(\omega)$, $\lambda_{Sj}(\omega)$, $\lambda_{Tk}(\omega)$ are continuous with ω. Note that mode index (number of voltage nodes in a segment) is *not* continuous on a given continuity branch: for a single segment RFQ, index jump may be 1 (resp. 2) when one (resp. both) end load go through infinity. Problem solutions are finally obtained by solving the 3 sets of *characteristic equations*

$$\lambda_{Qi}(\omega) = (\omega/c)^2,\ \lambda_{Sj}(\omega) = (\omega/c)^2,\ \lambda_{Tk}(\omega) = (\omega/c)^2.$$

Numerical Inputs to the Model.

First, dipole modes voltages have been measured in the 300-600 MHz range for each RFQ segment. s_a, s_b and mode index are obtained by fitting cosine function (Gauss-Newton-Levenberg-Marquardt non-linear least-squares) to measured voltage, and σ_a, σ_b by 3rd degree polynomial fit (Figure 3). Anti-resonances of rods are found to be close to quarter-wavelength, with $L_{Rod}/\lambda = 0.220 \pm 0.005$ (Figure 4). In Table 1, quadrupole modes are computed with constant BC, and show the regular progression of mode index n, as predicted by Sturm's alternation theorem. Dipole modes are computed with dispersive BC: clearly the alternation theorem no more applies, and two more modes show up in the 300-600 MHz band.

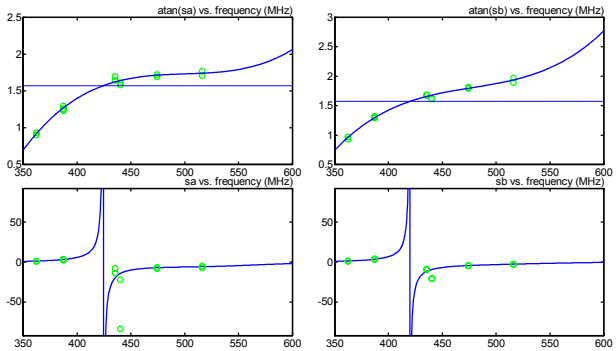

Figure 3: BC fit vs. frequency (350 to 600 MHz) for segment ca_x; left: end 1, right: end 2; top: σ functions; bottom: s functions. Dots: measurements, lines: fit. Rod lengths 155 mm.

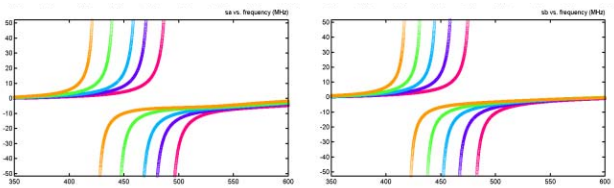

Figure 4: s fit vs. frequency (350 to 600 MHz) for segment ca_x; End 1 at left: rod lengths 135, 140, 144, 150 and 155 mm (right to left). End 2 at right: rod lengths 135, 140, 145, 150 and 155 mm (right to left).

Table 1: Eigen-frequencies and mode index of ca_x segment, with 155 mm rods at both ends. *signal-to-noise ratio too low for proper index identification

	Dipole eigen-modes				Quadrupole eigen-modes			
	Bead-pull		Model		Bead-pull		Model	
#	MHz	n	MHz	n	MHz	n	MHz	n
1	337.35	0	337.18	0	348.75	0	350.83	0
2	343.05	1	342.41	1	355.95	1	358.70	1
3	362.10	2	361.89	2	378.75	2	381.33	2
4	387.00	3	388.14	3	411.60	3	416.30	3
5	411.60	*	413.10	4	458.40	4	460.79	4
6	435.15	3	437.90	3	504.45	5	512.27	5
7	474.00	4	472.92	4	567.30	6	568.81	6
8	516.00	5	519.03	5				
9	571.95	6	568.55	6				

STABILITY ANALYSIS

Let C_1, C_2, C_3, C_4 be the inter-vane capacitances per unit length, and let's define C_{QQ}, C_{SQ}, C_{TQ} and C_{SSTT} by

$$C_1 := C_{QQ} + C_{SQ} + C_{SSTT},\ C_2 := C_{QQ} - C_{TQ} - C_{SSTT},$$
$$C_3 := C_{QQ} - C_{SQ} + C_{SSTT},\ C_4 := C_{QQ} + C_{TQ} - C_{SSTT}.$$

Analysis shows that C_{QQ}, C_{SQ}, C_{TQ} perturbations induce first order perturbations of resp. the Q, S and T components of voltage. C_{SSTT} induces second order perturbations, which are neglected. Assume $dC_{QQ}(z) = \Delta C_{QQ}.\delta(z-z_0)$, where δ is the Dirac distribution. The resulting voltage perturbation of some Q-mode V_{Qi} is $dV_{Qi}(z) = |(dV_{Qi})_Q,0,0|$. Define function $h_{QQ}(z,z_0)$ and norm $\|h_{QQ}\|$ by

$$\frac{dV_{Qi}(z)_Q}{V_{Qi}(z)} = h_{QQ}(z, z_0)\frac{\Delta C_{QQ}}{C_{QQ}(z_0)} \le \|h_{QQ}\|\frac{\Delta C_{QQ}}{C_{QQ}(z_0)},$$

with similar definitions for $\|h_{SQ}\|$ and $\|h_{TQ}\|$. Note that using quadrant inductances for the analysis would lead to virtually identical quantities. $\|h_{QQ}\|$ is minimized by selecting the optimum value of coupling capacitance C_C (here 1 pF, which required additional 0.8 mm shims to be added on either side of coupling plates), and $\|h_{SQ}\|$, $\|h_{TQ}\|$ by choosing proper end loads (here matched), given optimum C_C (Figure 5).

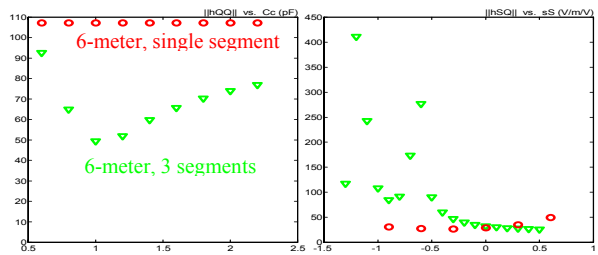

Figure 5: Stability analysis of 3-segment RFQ model.

Table 2: Dipole rod tuning summary

L_{Rod}	ca_x	x_be_x	x_df
135	-25.05	-32.35	+20.46
140	-30.10	-34.41	0
145	-38.23	-38.22	-23.60
150	-44.90	-45.66	-33.36
155	-52.69	-52.67	-42.50
160	-60.02	-59.43	-49.96
required	-50.58	-50.00	-50.58
tuned L_{Rod}	152	152	155*

* preferred to 160 for mechanical stability.

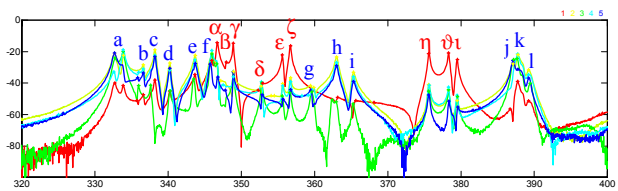

Figure 6: RFQ resonances after rod tuning and segment assembly. Quadrupole (red) and dipole excitations.

a	D 0–0–0	h	D 2+1–2	γ	Q 0+0+0
b	D 0–1–0	i	D 2+2+2	δ	Q ?±?±?*
c	D 0+0+0	j	D 3–3±?*	ε	Q 1+1–1
d	D 1–1–1	k	D 3±3±?*	ζ	Q 1+1+1
e	D 1+1–1	l	D 3±3±?*	η	Q 2–2–2
f	D 1+1+1	α	Q 0–0–0	ϑ	Q 2+1–2
g	D 2–2–2	β	Q 0–1–0	ι	Q 2+2+2

* signal-to-noise ratio too low for discrimination.

DIPOLE RODS TUNING

Most critical for dipole component stability is D_1 mode, because D_{1+1+1} is closest to accelerating Q_{0+0+0}. Quadratic separation $\varphi = \text{sign}\,[f_{D1}-f_{Q0}]\,.\,\text{sqrt}\,|f_{Q0}^2 - f_{D1}^2|$ has been measured vs. L_{Rod} for each segment, and L_{Rod} is interpolated for the required φ computed from model (Table 2). Figure 6 shows the spectrum of coupled structure, with modes distributed as expected.

SLUG TUNERS

Tuners are modelled by stepped parallel inductance functions, having one "rectangular pulse" per slug. The line model relates the space of inductance perturbations (via the A matrix), to the space of voltage perturbations. First order perturbation analysis shows that eigen-functions are a basis for voltage perturbation space; inductance basis functions can be built, having a one-to-one correspondence with the V_{Qi}, V_{Sj}, V_{TK}. The tuning process is then straightforward: first, measure RFQ voltage, compute error relative to objective, and expand error in the voltage basis. Use transfer function to transform voltage coefficients into inductance coefficients. Apply these to inductance basis functions, eventually with some gain coefficient, sum for each slug, and apply to RFQ. Several iterations of this process are usually necessary, since an eigen-problem is essentially non-linear.

Twenty-six tuners per quadrant are used to tune the 6-meter RFQ model, so there are 26 inductance basis functions in each subset (Figure 7). Note that dummy RF ports are included to achieve stable sampling.

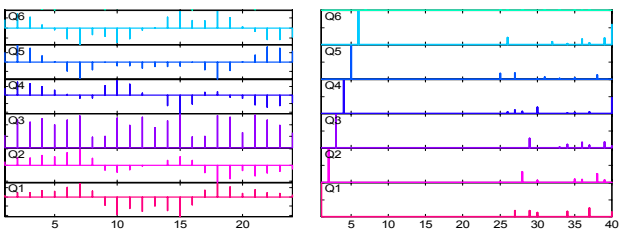

Figure 7: Left: first six inductance basis functions of the Q-subset vs. abscissa; right: spectra vs. mode index. Spectral purity is perfect in the subspace spanned by the 26 first eigen-modes. Some aliasing due to sampling is visible at higher indices.

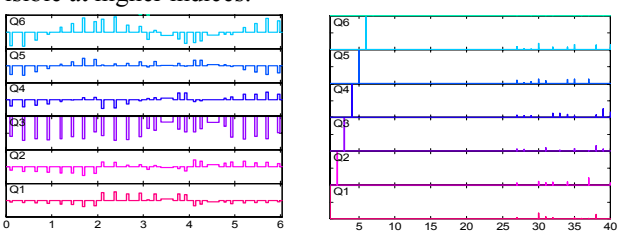

Figure 8: Left: first six filter sequences of the Q-subset vs. sample index; right: transmittances vs. mode index. Transmittance of filter channels is perfect in the subspace spanned by the 24 first eigen-modes. Some aliasing due to sampling is visible at higher indices.

Voltages are derived from bead-pull measurements of quadrants magnetic field. A small fraction only of the 2001 samples acquired along the RFQ is usable, because of 3D local effects close to slugs, segment ends, etc. Linear sampling filters are used to derive voltage basis coefficients from measured samples. Sampling stability is highly conditioned by the number and positions of range samples; here 24 samples are used to build a 24-channel filter (Figure 8).

CONCLUSION

A total number of six iterations was enough to reduce voltage errors within ±1% (Table 3, Figure 9-left). Loop gain was set to 0.8, and bandwidth to 3 x 12 modes, in order to reject high-frequency noise. Figure 9-right shows that spurious components are at least 45 dB down the accelerating component, the loop being able to reduce major components by at least 30 dB. No spectral re-growth was found above pass-band (indices > 12).

Table 3: Tuning performance.

	un-tuned	tuned
f_{Q0+0+0}	348.897 MHz	351.979 MHz
Q	−31. ~ +45 %	−1.30 ~ +1.00 %
S	−7.1 ~ +19 %	−0.86 ~ +0.56 %
T	−32. ~ +22 %	−0.76 ~ +1.18 %

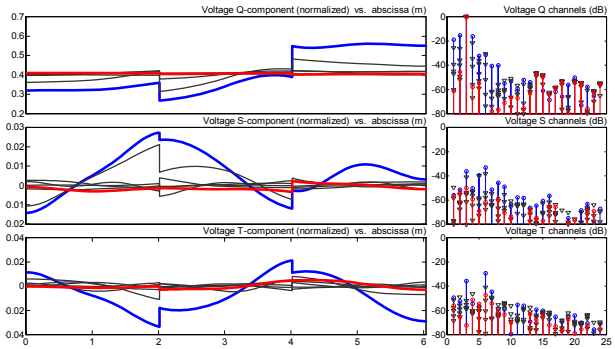

Figure 9: Left: Q, S and T components of accelerating mode Q_{0+0+0} vs. abscissa; blue: un-tuned, red: tuned, black: intermediate steps. Curves are normalized according to $\int V_Q^2\,dz = 1$. Right: spectral coefficients of Q, S and T components (dB) vs. mode index.

REFERENCES

[1] F. Simoens, A.C. France, "A fully distributed test bench for the measurement of the field distribution in RFQ and other resonant cavity", EPAC2002.

[2] A.C. France, F. Simoens, "Theoretical analysis of a real-life RFQ using a 4-wire model and the theory of differential operators", EPAC2002.

[3] C.G. Gal, "Sturm-Liouville operator with general boundary condition", Electronic Journal of Differential Equations, Vol. 2005, No. 120, pp1-17.

[4] W.J. Code, P.J. Browne, "Sturm-Liouville with boundary condition depending quadratically on the eigen-parameter", Mathematical Sciences Group, Saskatchewan University (Canada), 2004.

[5] J.E. Storer, "Passive network synthesis", Ch. 3, McGraw-Hill, 1957.

[6] G.C. Temes, S.K. Mitra, "Modern filter theory and design", Ch. 7, John Wiley & Sons, 1973.